ANALYTICAL SCIENCES JULY 2017, VOL. 33

Direct Electron Transfer-type Bioelectrocatalysis of Peroxidase at Mesoporous Carbon Electrodes and Its Application for Glucose Determination Based on Bienzyme System

Hong-qi XIA, Yuki KITAZUMI, Osamu SHIRAI, and Kenji KANO†

Division of Applied Life Sciences, Graduate School of Agriculture, Kyoto University, Kyoto 606–8502, Japan

Non-catalytic direct electron transfer (DET) signal of Compound I of horseradish peroxidase (POD) was first detected at 0.7 V on POD/carbon nanotube mixture-modified electrodes. Excellent performance of DET-type bioelectrocatalysis was achieved with POD immobilized with glutaraldehyde on Ketjen Black (KB)-modified electrodes for H_2O_2 reduction with an onset potential of 0.65 V (*vs.* Ag|AgCl|sat. KCl) without any electrode surface modification. The POD-immobilized KB electrode was found to be suitable for detecting H_2O_2 with a low detection limit (0.1 μM at $S/N = 3$) at –0.1 V. By co-immobilizing glucose oxidase (GOD) and POD on the KB-modified electrode, a bienzyme electrode was constructed to couple the oxidase reaction of GOD with the DET-type bioelectrocatalytic reduction of H_2O_2 by POD. The amperometric detection of glucose was performed with a high sensitivity (0.33 ± 0.01 μA cm^{-2} μM^{-1}) and a low detection limit (2 μM at $S/N = 3$).

Keywords Direct electron transfer, peroxidase, glucose oxidase, glucose biosensor

(Received March 3, 2017; Accepted March 27, 2017; Published July 10, 2017)

Introduction

Peroxidases (POD) are ubiquitous in the living world. The catalytic center of POD is a protoheme at which hydrogen peroxide (H_2O_2) is reduced to water in the presence of suitable electron donors. The ferric state of POD is oxidized to Compound I by H_2O_2 in a one-step two-electron reaction:

$$\mathrm{POD(Fe^{3+}) + H_2O_2 \longrightarrow Compound\ I + H_2O} \quad (1)$$

Compound I is re-reduced to the ferric state *via* Compound II as an intermediate:

$$\mathrm{Compound\ I + H^+ + e^- \longrightarrow Compound\ II} \quad (2)$$

$$\mathrm{Compound\ II + H^+ + e^- \longrightarrow POD(Fe^{3+})} \quad (3)$$

The electrochemistry of horseradish POD has been extensively studied.[1] H_2O_2 is not the exclusive electron acceptor to provide Compound I from the ferric state. Actually, the ferric form is easily oxidized to Compound I (as well as Compound II) by suitable electron acceptors such as $IrCl_6^{2-}$. The three redox states are reversible and the formal potential of the reactions given by Eqs. (2) and (3) were spectroelectrochemically determined as 0.75 and 0.72 V (*vs.* Ag|AgCl at pH 7.0), respectively.[2] Since the electrochemical oxidation of H_2O_2 frequently requires high electrode potentials in the absence of catalysts, the situation leads to co-oxidation of other electroactive metabolites in the physiological fluids to cause positive interference. Therefore, POD is frequently used in biosensors for determination of H_2O_2.

Many papers have reported non-catalytic direct electron transfer (DET) of POD and bioelectrocatalytic reduction of H_2O_2.[3-6] However, most non-catalytic DET signals of POD are assigned to the redox reaction of Fe^{3+}/Fe^{2+} of the protoheme at –0.2 V (*vs.* Ag|AgCl) and the Fe^{3+}/Fe^{2+} redox reaction is entirely unrelated to the catalytic redox cycle described in Eqs. (1) – (3). In addition, the current densities of the catalytic waves of the H_2O_2 reduction at POD-adsorbed electrodes are very low, and the onset potentials are in a large variety in the literature and are usually much more negative than the redox potential of Compound I. Therefore, several artificial mediators have been proposed for the reduction of Compound I to construct mediated electron transfer- (MET-)type biosensors for H_2O_2 detection.[7,8] MET-type POD sensors have been frequently combined with an H_2O_2-generating oxidase for determination of the first substrate of the oxidase.[9-15] One of the issues to be considered for such MET-type POD/oxidase bienzyme-electrode reactions may be that the oxidized form of a mediator generated in the POD reaction frequently works as an electron acceptor of the oxidase in the bienzyme system (due to the dehydrogenase activity),[13] which results in negative interferences.

Recently, catalytic waves of H_2O_2 reduction by POD on electrodes with positive onset potentials of approximately 0.5 – 0.6 V (*vs.* Ag|AgCl) were reported at carbon nanotube-(CNT-)modified graphite electrodes, although the mechanism remains unclear.[16,17] It has been proposed that mesoporous structures with porous radii close to the radius of an enzyme[18-20] and electrostatic interaction between the redox center of an enzyme and an electrode surface[21-26] are important to improve

† To whom correspondence should be addressed.
E-mail: kano.kenji.5z@kyoto-u.ac.jp

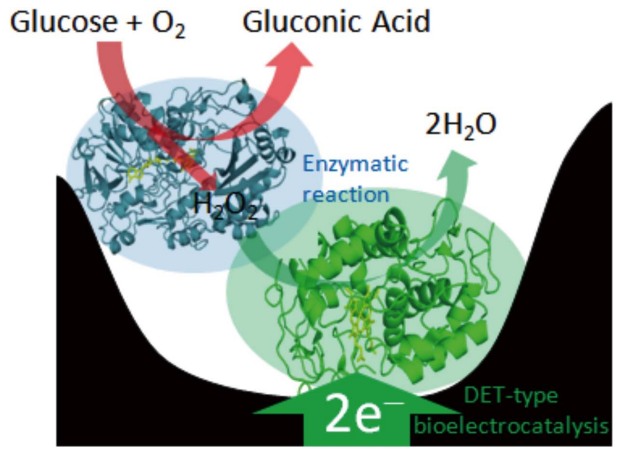

Scheme 1 Proposed DET-type bienzymatic mesoporous electrode for glucose determination.

the performance of DET-type bioelectrocatalysis. Therefore, there seems to be some possibility to construct mesoporous electrodes suitable for DET reaction of POD.

On the other hand, glucose oxidase (GOD) is one of the key enzymes for determination of glucose. Although there are a countable number of papers claiming DET-type bioelectrocatalysis of GOD, a recent conclusion is that native GOD does not undergo DET reaction.[27] Therefore, GOD-based biosensors should detect H_2O_2 generated in the oxidase reaction or the reduced mediator in MET-type bioelectrocatalysis of GOD using its dehydrogenase activity.

In this work, Ketjen Black (KB) and water-soluble CNTs were used to construct mesoporous structured carbon electrodes suitable for DET-type bioelectrocatalysis of POD. As a result, a pair of weak but clear waves of non-catalytic DET reaction of POD embedded in CNTs was for the first time recorded at a POD/CNT mixture-modified electrode. In addition, great performance of mediator-free DET-type bioelectrocatalysis of POD was realized for two-electron reduction of H_2O_2 at KB-modified electrodes without any special electrode surface modification. The high catalytic efficiency and high stability of POD-immobilized KB-modified electrodes was useful to reductively detect H_2O_2. In addition, the POD-electrode was used to detect H_2O_2 generated in the GOD reaction to construct semi-DET-type bienzyme biosensor for glucose determination, as shown in Scheme 1.

Experimental

Materials and reagents

Ketjen Black EC300J (KB) was donated by Lion Co. (Japan). Poly(tetrafluoroethylene) fine powder (PTFE, 6-J) was obtained from DuPont Mitsui Fluorochemicals (Japan). Water-dispersed carbon nanotubes (CNT, outer diameter: 10 – 15 nm, length: 1 – 4 μm) were donated by Nitta Corp. (Japan). Ascorbic acid (AA), uric acid (UA), glutaraldehyde (GA, 20%), glucose, and H_2O_2 were obtained from Wako Chemicals Co. (Osaka, Japan). Peroxidase from horseradish (POD, EC 1.11.1.7, 292 U mg^{-1}) and glucose oxidase from *Aspergillus sp*. (GOD, EC 1.1.3.4, 163 U mg^{-1}) were purchased from Toyobo Co. (Japan) and used without further purification. UA solution was prepared with 0.1 M KOH (1 M = 1 mol dm^{-3}), and the enzymes, substrates, AA, and GA solutions were prepared with a 0.1 M phosphate buffer (pH 7.0). All other chemicals used in this study were of analytical grade and all solutions were prepared with distilled water.

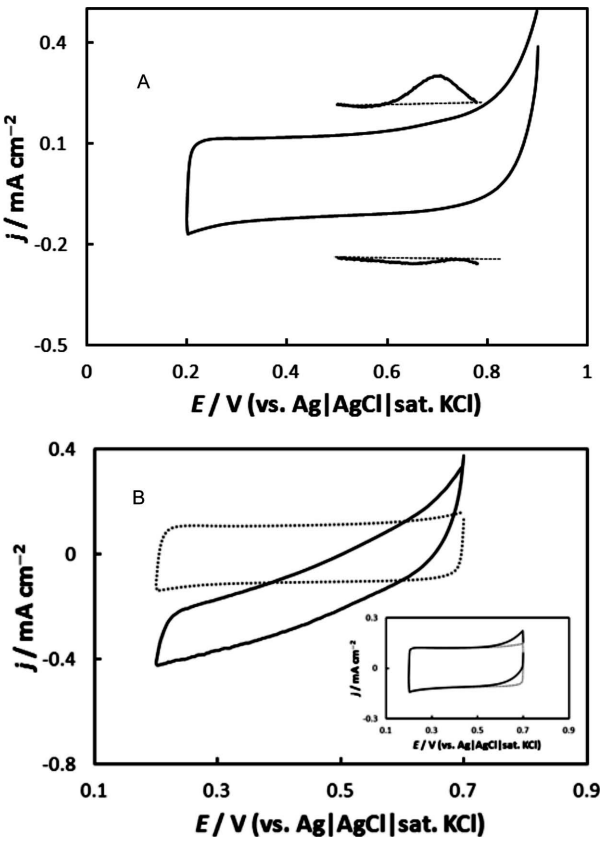

Fig. 1 A) Non-catalytic CV of POD/CNT mixture-modified GCE in the absence of H_2O_2 in 0.1 M phosphate buffer (25°C, pH 7) at a scan rate of 5 mV s^{-1}. The redox waves are shown after the capacitive background signal subtraction and are multiplied by a factor of 15 for the sake of clarity. B) Rotating disk CVs of POD/CNT mixture-modified GCE in the absence (dotted line) and presence (solid line) of 0.1 mM H_2O_2. The inset shows rotating disk CVs at CNT-modified GCE in the absence and presence of 0.1 mM H_2O_2.

Preparation of POD modified electrode and POD/GOD bienzyme-modified electrode

A KB-modified glassy carbon electrode (KB/GCE) was prepared according to a previously described method.[28] In brief, a 3-μL KB slurry (PTFE:KB = 1:4, w/w) was dropped onto a rotating disk GCE surface (diameter = 3 mm) and dried at room temperature (1 L = 1 dm^3). For enzyme immobilization, a 20-μL enzyme solution (POD: 5 mg mL^{-1}) containing 5% (w/v) of GA was applied on the KB/GCE and dried at room temperature for 2 h. The electrode was washed with a phosphate buffer (0.1 M, pH 7.0) and used for electrochemical measurements.

When CNTs were used as a platform for enzyme immobilization, the POD solution was mixed with a water soluble CNT suspension (0.3%) to form a POD/CNT mixture (POD:CNT = 1:2, w/w). A 20-μL POD/CNT mixture was applied on a polished GCE and dried under reduced pressure at room temperature for 30 min. This is a new method for enzyme immobilization using CNTs without any reagents. CNTs would be immobilized on GCE with π-π stacking and also seem to enfold the enzyme to minimize the length between the redox

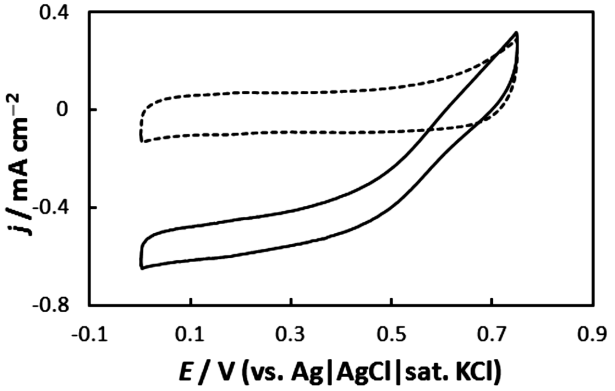

Fig. 2 Rotating disk CVs at POD immobilized KB/GCE in the absence (dotted line) and in the presence (solid line) of 0.1 mM H_2O_2 in 0.1 M phosphate buffer (25°C, pH 7) at a scan rate of 5 mV s^{-1} and a rotating rate of 4000 rpm.

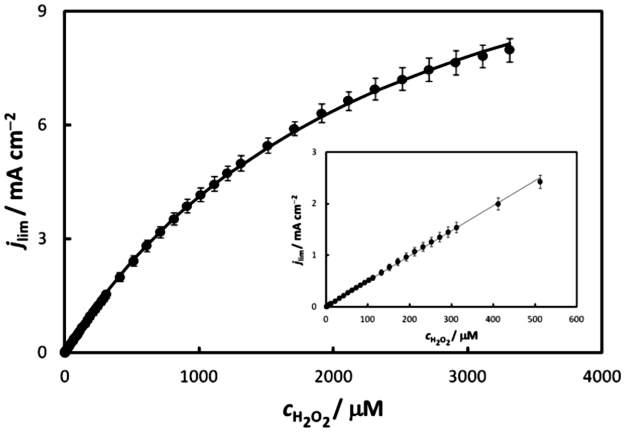

Fig. 3 Dependence of the limiting steady-state current response (j_{lim}) on the concentration of H_2O_2 ($c_{H_2O_2}$) at 0 V. The solid line was evaluated by a nonlinear regression analysis with Eq. (4), and the inset shows a linear dependence of j_{lim} on $c_{H_2O_2}$ at low $c_{H_2O_2}$. All measurements were carried out with a POD-immobilized KB/GCE in 0.1 M phosphate buffer (25°C, pH 7) at a rotating rate of 4000 rpm.

center of the enzyme and a CNT.

For the POD/GOD bienzyme-modified electrode, a 20-μL enzyme solution containing POD, GOD, and GA was applied on a KB/GCE surface and dried for 2 h at room temperature. For long-term storage, the enzyme electrode was stored at 4°C in a water-saturated atmosphere.

Electrochemical measurement

Cyclic voltammetry and chronoamperometry were performed using an electrochemical analyzer ALS 701 E with a rotating disk GCE as a working electrode, a Pt wire as a counter electrode, and an Ag|AgCl|KCl (sat.) electrode as a reference electrode. Rotating disk voltammetry was performed at a rotating rate of 4000 rpm to obtain steady-state currents. All potentials were referenced against the reference electrode.

Results and Discussion

Non-catalytic and catalytic DET-type signals POD on mesoporous carbon electrodes

Figure 1A shows a cyclic voltammogram (CV) of a POD/CNT mixture-modified GCE in a 0.1 M phosphate buffer solution (25 ± 1°C, pH 7.0). A pair of small but visible surface-confined redox waves of POD was observed. The midpoint potential is approximately 0.7 V and very close to the average (0.73_5 V) of the two redox potentials determined spectroelectrochemically for the reactions of Eqs. (2) and (3).[2] The negative shift of the midpoint potential indicates that Compound I is embedded in CNTs more stably than the ferric form, most probably due to electrostatic interaction of Compound I with negatively charged CNTs. This is the first report of a non-catalytic DET signal of POD. In the presence of H_2O_2, a steady-state catalytic wave of H_2O_2 reduction was observed at potentials more negative than 0.6 V on a rotating disk CV (Fig. 1B). As expected, no catalytic reduction wave was observed in the absence of POD (Fig. 1B, inset) and at a POD-immobilized GCE (Fig. S1, Supporting Information). Therefore, the reduction wave is assigned to a DET-type bioelectrocatalytic reduction of H_2O_2 by POD embedded in CNTs. Because direct oxidation currents of H_2O_2 were observed at potentials more positive than 0.6 V (Fig. 1B), the zero current potential (0.6 V) is determined by the POD-catalyzed reduction of H_2O_2 and the non-catalytic direct oxidation of H_2O_2. This is the reason why the zero current potential is slightly more negative than the midpoint potential of POD (Compound I) embedded in CNTs.

Figure 2 shows rotating disk CVs at a POD-immobilized KB/GCE in a 0.1 M phosphate buffer solution in the absence and presence of H_2O_2. A well-defined sigmoidal catalytic reduction wave was obtained with an onset potential of approximately 0.65 V. The steady-state current density reached a limiting value of 0.7 ± 0.1 mA cm^{-2} at 0.1 mM H_2O_2. The signal was very stable even at a high rotating rate (4000 rpm) because POD is stably immobilized in the mesoporous structure of KB/GCE. Since the potential window of KB/GCE was limited to *ca.* 0.5 V (Fig. S2, Supporting Information), it was impossible to detect a non-catalytic DET signal of POD immobilized on the KB/GCE. However, very fast electron transfer from KB to Compound I must occur compared with CNTs, because the rising portion of the catalytic wave is sharper at KB/GCE than that at CNT/GCE. The limiting current density is also larger at KB/GCE than that at CNT/GCE. The three dimensional *meso*/micro structures of KB on the GCE seem to be one of the most important factors in improving the performance of the DET-type bioelectrocatalysis of POD, as predicted in our previous studies.[18-20] The fast catalytic reduction of H_2O_2 was realized at the POD-immobilized KB/GCE without any extra mediator or special surface modification at such high potentials.

We used GA as a cross-linker to form a stable enzyme layer for DET-type bioelectrocatalysis. Such DET-type catalytic H_2O_2 reduction wave was obtained at POD-modified KB/GCE electrode in the absence of GA. However, the current decreased with time, and the catalytic current density was smaller than that in the presence of GA. If multi-layer POD molecules are formed on the electrodes when GA is used, POD molecules in the second and upper layers (if any) would not work as DET-type electrocatalysts.

Figure 3 shows the relationship between the limiting reduction current density (j_{lim}) at the POD/KB/GCE and the H_2O_2 concentration ($c_{H_2O_2}$). The value of j_{lim} was measured at 0 V. The j_{lim} value increased almost linearly with $c_{H_2O_2}$ up to 0.5 mM and showed a Michaelis–Menten-type curved characteristic at increased $c_{H_2O_2}$:

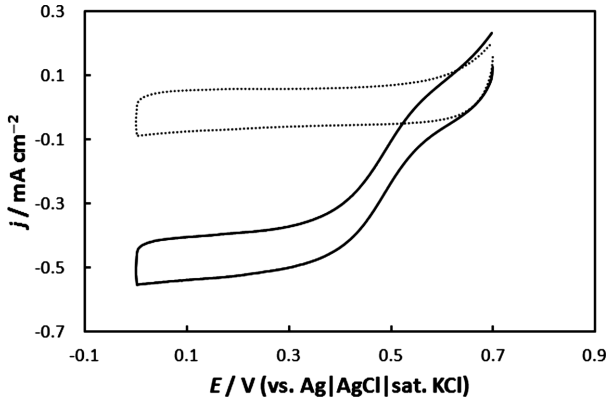

Fig. 4 Rotating disk CVs at GOD/POD-immobilized KB/GCE in the absence (dotted line) and in the presence (solid line) of 1 mM glucose in 0.1 M phosphate buffer (25°C, pH 7) at a scan rate of 5 mV s^{-1} and a rotating rate of 4000 rpm.

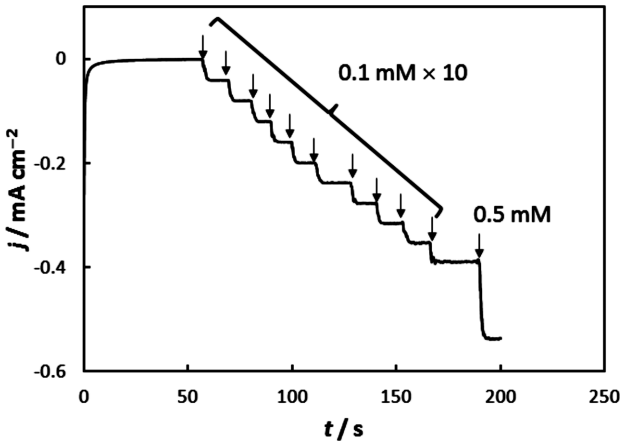

Fig. 5 Steady-state current response at the rotating GOD/POD-immobilized KB/GCE upon the successive addition of glucose at 0 V. The measurement was carried out in 0.1 M phosphate buffer (25°C, pH 7) at a rotating rate of 4000 rpm.

$$j_{\mathrm{lim}} = \frac{j_{\mathrm{lim,max}}}{1 + K_{\mathrm{M,app}}/c_{\mathrm{H_2O_2}}}, \quad (4)$$

where $j_{\mathrm{lim,max}}$ and $K_{\mathrm{M,app}}$ represent the maximum value of j_{lim} and the apparent Michaelis–Menten constant, respectively. Using $j_{\mathrm{lim,max}}$ and $K_{\mathrm{M,app}}$ as adjustable parameters, the data were fitted to Eq. (4) through a non-linear regression analysis with Gnuplot© 5.0. The refined $K_{\mathrm{M,app}}$ of POD immobilized on the KB/GCE was 2.4 ± 0.6 mM. The detection limit of H_2O_2 with the POD/KB/GCE was as low as 0.1 μM ($S/N > 3$), and the linear range was from 0.5 to 500 μM with a slope of 4.8 ± 0.4 μA cm^{-2} μM^{-1}. The biosensor prepared has high sensitivity and is suitable for the detection of extremely low concentrations of H_2O_2.

GOD/POD bienzyme-immobilized electrode for glucose determination

Figure 4 shows typical rotating-disk CVs obtained at a GOD/POD-immobilized KB/GCE in the presence and absence of glucose. A clear catalytic reduction wave was observed at the bienzyme electrode in the presence of glucose. As expected, the similar reduction wave was also obtained at the GOD/POD-immobilized KB/GCE when H_2O_2 was added (Fig. S3, Supporting Information). Such reduction wave was not observed in the absence of either POD or GOD on the electrode even in the presence of glucose. These results indicate that the reduction wave at the GOD/POD-immobilized KB/GCE is ascribed to the reduction of H_2O_2 (Eqs. (1) - (3)) generated in the GOD-catalyzed two-electron reduction of O_2 with glucose as an electron donor.

Figure 5 shows a typical current–time curve at the GOD/POD-immobilized KB/GCE with the successive addition of a glucose solution into an air-saturated buffer solution at a detection potential of 0 V. The catalytic current density increased with the addition of glucose and reached a steady-state within 2 s. Such fast response may be attributed to two factors: 1) the excellent electron-transfer kinetics from the KB-modified electrode to POD (Compound I), and 2) the fast mass-transfer of H_2O_2 generated by the GOD reaction in the immobilized bi-enzyme layer.

Considering the fact that the composition of POD and an H_2O_2-generated oxidase may affect the biosensing performance of bienzyme biosensors,[11,12] the ratio of POD to GOD was examined. Figure S4 (Supporting Information) shows the effects of the POD/GOD ratio on the relative current response to 1 mM glucose (ratios from 0.05 to 0.30 at a constant GOD concentration of 5 mg mL^{-1}) in the mixed enzyme/reagent solutions for immobilization. The relative response increased with the POD/GOD ratio and reached a maximum at a POD/GOD ratio (w/w) of 0.15. Then, it gradually decreased with increasing the POD/GOD ratio. Therefore, a POD/GOD ratio (w/w) of 0.15 was selected for the following experiments to obtain optimal sensitivity. The value was simply optimized here, but it would become very important in near future to describe the situation by numerical simulation based on the kinetics and the mass transfer of the substrate, O_2, and H_2O_2.

The effect of the detection potential was also investigated in the range from –0.2 to 0.2 V on the response of the biosensor in the presence of 1 mM glucose (Fig. S5, Supporting Information). With decreasing the detection potential from 0.2 V, the reduction current gradually increased and reached a maximum at –0.1 V. For more negative detection potential values (such as –0.2 V), the current decreased, probably because of the progressive inactivation of POD.[10] In addition, at potentials more negative than –0.15 V, the influence of non-catalytic direct reduction of O_2 at electrodes appeared. On the other hand, several reduced compounds such as AA and UA will be non-catalytically oxidized at carbon electrodes at potentials more positive than 0 V and interfere with the amperometric detection of glucose. Thus, the detection potential was set at –0.1 V for the glucose-sensing bienzyme electrode.

Glucose sensing

The characteristics of the biosensor were investigated by chronoamperometric measurements under the optimum conditions obtained above. Figure S6 (Supporting Information) shows a calibration curve. The data showed a linear dependence of the limiting catalytic current density on the glucose concentration (c_{glc}) from 5 to 1500 μM and a Michaelis–Menten-type relation at increased c_{glc}. The apparent Michaelis–Menten constant ($K_{\mathrm{M,app}}$) for glucose was estimated to be 3.5 ± 0.3 mM, which is much lower than the true Michaelis constant reported for GOD (33 mM with O_2 as an electron acceptor in a solution under air-saturated conditions).[29] This is most probably because of the lower $K_{\mathrm{M,app}}$ value (2.4 ± 0.6 mM) of POD against H_2O_2 than that of GOD against glucose. The lowest glucose detection

limit with the proposed bienzyme biosensor was estimated at 2 μM ($S/N > 3$) with a slope of 0.33 ± 0.01 μA cm^{-2} μM^{-1}.

GOD shows highly specific catalytic activity toward glucose even in the presence of other carbohydrates. However, some interferences such as AA may react with POD (Compound I) as electron donors resulting in negative interferences.[30] The effects of the presence of UA (0.5 mM) and AA (0.5 mM) as probable interfering species on glucose detection were examined. These compounds caused negligible decreases of less than 1 and 2%, respectively, for the reduction current of 0.5 mM glucose. Therefore, these substances hardly interfered with the response of the biosensor due to low detection potential and high specificity of the enzymes.

In addition, the stability of the proposed bienzyme biosensor was investigated with chronoamperometry at –0.1 V for 7200 s. Only a slight decrease (<8%) in the current response (at 0.5 mM glucose) was observed for the continuous measurements. For long-term storage stability, the prepared biosensor was stored at 4°C for two weeks. The current response to 0.5 mM glucose still remained above 90%. The results verify the high stability of the bienzyme biosensor.

The low detection limit and high stability is suitable for glucose determination in real samples, for example, in serum. Since the glucose concentration in human serum (c_{glc} = 4.4 – 6.6 mM)[31] is higher than the upper limit of the linear range, we supposed to detect glucose in a diluted serum sample. Therefore, glucose determination was performed in a phosphate buffer (pH 7) containing 1 mg mL^{-1} bovine serum albumin (BSA) as a diluted serum mimic. The current responses were recorded with the successive addition of a standard glucose solution. Figure S7 (Supporting Information) shows the relationship between j_{lim} and c_{glc}. The slope (0.31 ± 0.03 μA cm^{-2} μM^{-1}) was similar to that obtained for the standard glucose solution (0.33 ± 0.01 μA cm^{-2} μM^{-1}). The result indicates that the proposed bienzyme biosensor works properly even in the presence of BSA (1 mg mL^{-1}). Therefore, the proposed bienzyme biosensor is applicable for clinical diagnosis.

Conclusions

Thanks to the three-dimensional structure of mesoporous materials, a non-catalytic DET signal of POD was detected at the POD/CNT mixture-modified electrode with a redox potential of approximately 0.7 V. To the best of the authors' knowledge, this is the first case of the voltammetric detection of the non-catalytic wave of POD (Compound I). Great performance of DET-type bioelectrocatalysis of immobilized POD was realized at KB-modified electrodes without any surface modification at such positive electrode potentials up to 0.6 V. The POD-immobilized KB/GCE can be utilized for detecting H_2O_2 with a low detection limit and high sensitivity. GOD as an H_2O_2-generated oxidase was co-immobilized with POD on KB/GCE for glucose determination. The proposed bienzyme glucose biosensor showed high sensitivity and high stability.

The proposed bienzyme system can be applied to the detection of several substrates by just replacing GOD with the corresponding oxidase, such as D-amino acid oxidase,[11] sarcosine oxidase,[12] and glutamate oxidase.[14] In addition, the reduction of H_2O_2 at such high electrode potentials on POD-immobilized mesoporous carbon electrodes can be utilized as bio-cathodes in biofuel cells in place of multi-copper oxidase-based bio-cathodes, since the activity of the latter bio-cathodes are liable to be inhibited by H_2O_2 and halogen ions.[32,33] The positive onset potential for the H_2O_2 reduction at POD-immobilized electrodes is also one of the benefits as bio-cathodes in biofuel cells.

Acknowledgements

This work was supported in part by the scholarship of the Ministry of Education, Culture, Sports, Science and Technology, Japan (No. 201308210170), for researcher students from China to Japan (to H.-Q. X.). The authors would like to thank Lion Co. and Nitta Corp. and for their charitable contributions of KB and CNT, respectively. The authors would also like to thank Enago (www.enago.jp) for the English language editing.

Supporting Information

Additional electrochemical data and the calibration curves are provided in the Supporting Information. This material is available free of charge on the Web at http://www.jsac.or.jp/analsci/.

References

1. T. Ruzgas, L. Gorton, J. Emnéus, and G. Marko-Varga, *J. Electroanal. Chem.*, **1995**, *391*, 41.
2. M. Torimura, M. Mochizuki, K. Kano, T. Ikeda, and T. Ueda, *Anal. Chem.*, **1998**, *70*, 4690.
3. Y. D. Zhao, W. D. Zhang, H. Chen, Q. M. Luo, and S. F. Y. Li, *Sens. Actuators, B*, **2002**, *87*, 168.
4. Y. T. Kong, M. Boopathi, and Y. B. Shim, *Biosens. Bioelectron.*, **2003**, *19*, 227.
5. T. Gu, J. Wang, H. Xia, S. Wang, and X. Yu, *Materials*, **2014**, *7*, 1069.
6. K. Komori, T. Tatsuma, and Y. Sakai, *Langmuir*, **2016**, *32*, 9163.
7. T. Gu and Y. Hasebe, *Anal. Chim. Acta*, **2004**, *525*, 191.
8. R. Katsube,Y. Kitazumi, O. Shirai, M. Yamamoto, and K. Kano, *J. Electroanal. Chem.*, **2016**, *780*, 114.
9. L. Zhu, R. Yang, J. Zhai, and C. Tian, *Biosens. Bioelectron.*, **2007**, *23*, 528.
10. G. E. De Benedetto, F. Palmisano, and P. G. Zambonin, *Biosens. Bioelectron.*, **1996**, *11*, 1001.
11. C. H. Nieh, Y. Kitazumi, O. Shirai, and K. Kano, *Biosens. Bioelectron.*, **2013**, *47*, 350.
12. C. H. Nieh, S. Tsujimura, O. Shirai, and K. Kano, *Anal. Chim. Acta*, **2013**, *767*, 128.
13. R. Matsumoto, M. Mochizuki, K. Kano, and T. Ikeda, *Anal. Chem.*, **2002**, *74*, 3297.
14. S. Yoshida, H. Kanno, and T. Watanabe, *Anal. Sci.*, **1995**, *11*, 251.
15. M. Delvaux, A. Walcarius, and S. Demoustier-Champagne, *Biosens. Bioelectron.*, **2005**, *20*, 1587.
16. W. Jia, S. Schwamborn, C. Jin, W. Xia, M. Muhler, W. Schuhmann, and L. Stoica, *Phys. Chem. Chem. Phys.*, **2010**, *12*, 10088.
17. B. Reuillard, A. Le Goff, M. Holzinger, and S. Cosnier, *J. Mater. Chem. B*, **2014**, *2*, 2228.
18. Y. Sugimoto, R. Takeuchi, Y. Kitazumi, O. Shirai, and K. Kano, *J. Phys. Chem. C*, **2016**, *120*, 26270.
19. Y. Sugimoto, Y. Kitazumi, O. Shirai, and K. Kano, *Electrochemistry*, **2017**, *85*, 82.
20. K. Sakai, Y. Sugimoto,Y. Kitazumi, O. Shirai, K. Takagi, and K. Kano, *Electrochim. Acta*, **2017**, *73*, 85.

21. M. Tominaga, M. Ohtani, and I. Taniguchi, *Phys. Chem. Chem. Phys.*, **2008**, *10*, 6928.
22. Y. Sugimoto, Y. Kitazumi, S. Tsujimura, O. Shirai, M. Yamamoto, and K. Kano, *Biosens. Bioelectron.*, **2015**, *63*, 138.
23. H. Xia, Y. Kitazumi, O. Shirai, and K. Kano, *J. Electroanal. Chem.*, **2016**, *763*, 104.
24. H. Xia, K. So, Y. Kitazumi, O. Shirai, K. Nishikawa, Y. Higuchi, and K. Kano, *J. Power Sources*, **2016**, *335*, 105.
25. L. Peng, T. Utesch, A. Yarman, J. H. Jeoung, S. Steinborn, H. Dobbek, and F. W. Scheller, *Chem Eur. J.*, **2015**, *21*, 7596.
26. K. Monsalve, I. Mazurenko, C. Gutierrez-Sanchez, M. Ilbert, P. Infossi, S. Frielingsdorf, M. T. Giudici-Orticoni, O. Lenz, and E. Lojou, *ChemElectroChem*, **2016**, *3*, 2179.
27. G. Wilson, *Biosens. Bioelectron.*, **2016**, *82*, vii.
28. H. Xia, Y. Hibino, Y. Kitazumi, O. Shirai, and K. Kano, *Electrochim. Acta*, **2016**, *218*, 41.
29. B. E. P. Swoboda and V. Massey, *J. Biol. Chem.*, **1965**, *240*, 2209.
30. J. C. Deutsch, *Anal. Biochem.*, **1998**, *255*, 1.
31. G. Reach and G. S.Wilson, *Anal. Chem.*, **1992**, *64*, 381A.
32. R. D. Milton, F. Giroud, A. E. Thumser, S. D. Minteer, and R. C. Slade, *Chem. Commun.*, **2014**, *50*, 94.
33. C. Adam, P. Scodeller, M. Grattieri, M. Villalba, and E. J. Calvo, *Bioelectrochemistry*, **2016**, *109*, 101.